Hyperfine Interactions 47(1989)179–202

EDGE SPECTROSCOPY

G. WORTMANN

Institut für Atom- und Festkörperphysik, Freie Universität Berlin, D-1000 Berlin 33, Germany

Abstract

The near-edge X-ray absorption fine structure can provide information on the chemical form and local structure as well as on the electronic and even magnetic properties of the investigated systems on a microscopic (atomic) scale. Selected examples of the application of edge spectroscopy are presented with emphasis on the valence determination in rare-earth systems, where similar information can be obtained by Mössbauer spectroscopy.

1. Introduction

X-ray absorption spectroscopy (XAS) is known to provide structural information via the extended X-ray absorption fine structure (EXAFS). Misleadingly, the abbreviation "EXAFS" is often used for X-ray absorption spectroscopy, neglecting the fact that the near-edge fine structure independently contains a variety of valuable information on the investigated system. In the last decade, however, the near-edge X-ray absorption fine structure (NEXAFS or XANES) has been increasingly employed for studies of the electronic, chemical and structural properties of gaseous, liquid or solid systems on a microscopic (atomic) basis [1–6]. The near-edge structure of an absorption threshold monitors transitions of core electrons into unoccupied states. Some characteristic properties of this spectroscopy are listed in the following:

(i) It is specific to the absorbing atom and, thereby, provides information about the local properties.

(ii) The K-, $L_{I,II,III}$-, $M_{III,IV,V}$-edges allow only transitions into final states with defined orbital character, thus monitoring selectively the p, d, or f character of the unoccupied states.

(iii) Due to the E1 character of the photoabsorption process, strong polarization effects of the absorption edge are often observed, which can be fully exploited by using the linear-polarized synchrotron radiation and oriented absorbers with low symmetries.

This review will present selected examples on the application of edge spectroscopy, mostly performed in our laboratory. In rare-earth systems, for instance, L_{III}-edge spectroscopy has been widely applied for the study of valence transition as a function of pressure, temperature or chemical composition [7]. Here, we concentrate on systems where comparative studies with the Mössbauer effect were performed.

Edge spectroscopy has been successfully used for studying the orientation and bond lengths in molecular systems, for instance of molecules adsorbed on surfaces [8] or intercalated in polyacetylene and graphite. In such low dimensional systems, the polarization dependence of the edge spectra provides structural information in a simple way.

Finally, we want to draw attention to a new and exciting application of edge spectroscopy, namely the investigation of spin densities in magnetic systems by using circularly-polarized synchrotron radiation [9].

2. Methodological aspects

X-ray absorption spectroscopy measures the electronic absorption coefficient $\mu(E)$ of a sample. When going through an absorption threshold of an element contained in the absorber, the absorption cross section increases suddenly due to the additional absorption of the electrons contained in the respective K-, L_{I-III}-, M_{I-V}-,.. shell. The fine structure of the absorption edge, being most pronounced in the near-edge region and increasingly damped in the extended region of the threshold, contains the specific information on the absorbing atoms (fig. 1). There are some similarities in the experimental arrangements used in XAS and Mössbauer spectroscopy (see inset in fig. 1). X-ray tubes as photon sources, as used in the early days of XAS, are nowadays mostly replaced by synchrotron radiation. The energy of the photons is modulated by a monochromator, which is passed only by photons of a defined energy. Provided the energy of the threshold ($E \geqslant 2$ keV) is high enough to allow sufficient transmission through the absorber material (including windows), measuring in transmission geometry is preferred. Scattering geometry is used for the study of the absorption edges of the light elements, for very dilute systems, or for single-crystalline samples. In this case, the absorption is monitored by the yield of photoelectrons or of fluorescence X-rays. Since the flux of monochromated photons from an X-ray tube or from the synchrotron is not as constant as from a Mössbauer source, one needs two detectors for the photon flux: one for the intensity of the incoming photon flux, the other one for the flux of the transmitted photons or, in scattering geometry, the electron or fluorescence yield. Similar to the absorber thickness problem in Mössbauer spectroscopy, only homogeneous absorbers of appropriate thickness guarantee a reliable recording of the fine structure of the absorption edge. A full theoretical description of the near-edge spectra is complicated, but now increasingly applied [11]. In many applications of edge spectroscopy one uses just a fingerprint technique, e.g.

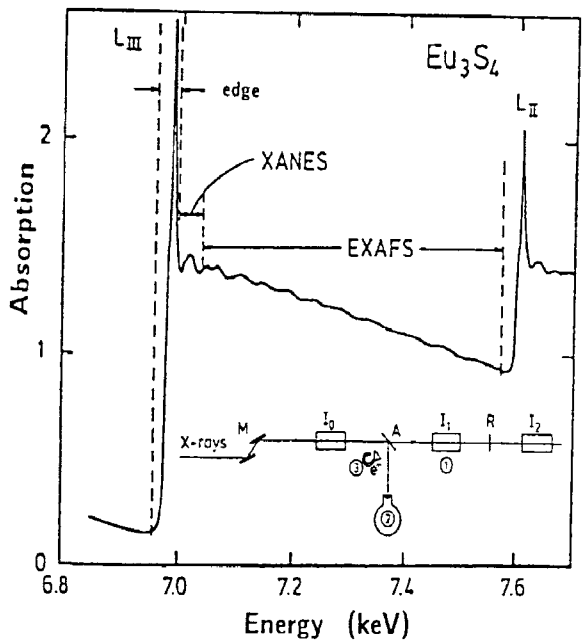

Fig. 1. X-ray absorption spectrum of Eu_3S_4 scanning the energy region between the L_{III}- and L_{II}-edge of Eu [10]. The range of the near-edge and extended X-ray absorption fine structure (XANES/edge and EXAFS, respectively) is indicated. The inset shows the principal experimental arrangement: Transmission geometry (1), scattering geometry with detection of fluorescent X-rays (2) and electrons (3); I_0, I_1, and I_2: ionization chambers, M: monochromator, A: absorber, R: reference absorber.

the comparison with reference systems, to derive information from the edge structure. For detailed information, we refer the reader to handbooks and recent conference proceedings [1–6].

3. Applications

3.1. VALENCE DETERMINATION IN RARE-EARTH SYSTEMS

(a) Integral valent systems / chemical shifts

Edge spectroscopy provides an easy tool to determine the valence in rare-earth (RE) systems as long as one is concerned with the heavier RE and is dealing with stable divalent and trivalent systems [7]. Since in this review we are interested in similarities and differences between edge spectroscopy and the Mössbauer effect, we have chosen Eu systems as examples where the isomer shift, as measured by the ^{151}Eu-Mössbauer resonance, provides complementary information on the valence state of the Eu ions.

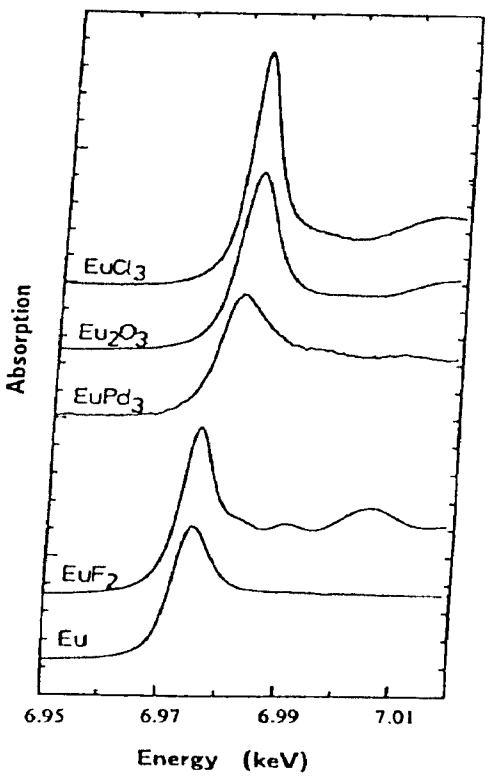

Fig. 2. Eu-L_{III} near-edge spectra of divalent and trivalent Eu compounds and metallic systems (from ref. [14]).

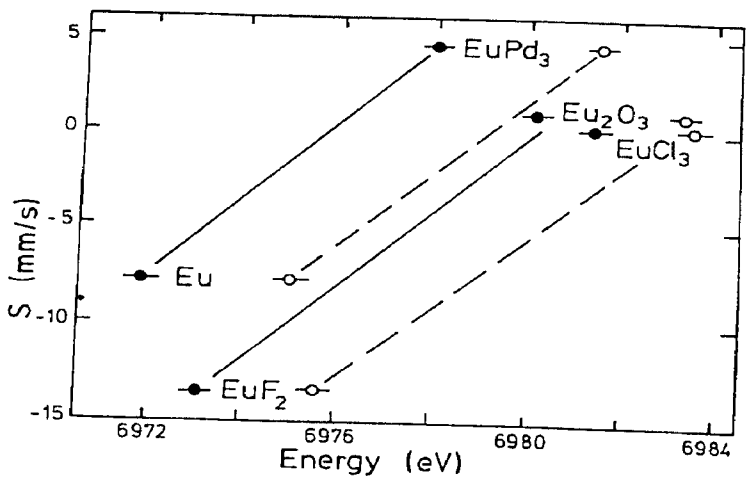

Fig. 3. Plot of ^{151}Eu isomer shifts versus the L_{III}-threshold energy for the Eu systems shown in fig. 2. Full dots represent the position of the edges, open dots the position of the white line (from ref. [14]).

The two valence states $Eu^{2+}(4f^7)$ and $Eu^{3+}(4f^6)$ can be easily distinguished by their different isomer shifts S [12,13]. The main reason for the difference, $\Delta S \cong 12$ mm/s, is, as well known since the early days of Mössbauer spectroscopy, the increased shielding of s-electron density by the additional 4f-electron in Eu^{2+} systems. For divalent as well as for trivalent Eu systems, the value of S may scatter considerably, e.g. from −14 mm/s for ionic Eu^{2+} compounds to −7 mm/s for metallic Eu^{2+} systems and from 0 to +4 mm/s for the corresponding Eu^{3+} systems.

Considering the edge spectroscopy, different valence states or, as in the RE case, different 4f-electron occupancies lead to different threshold energies of the respective K-, $L_{I,II,III}$-, and $M_{III,IV,V}$-edges. The basic reason for the different threshold energies is the lower binding energy of the respective core electrons caused by the shielding of the nuclear potential through the additional 4f-electron. Using the L_{III}-edge, as mostly done for the RE systems, the observed difference in the binding energy of the $2p_{3/2}$ electron is $\Delta E = U_{p\text{-}f} - U_{p\text{-}d} \cong 7$ eV for the heavier RE, where $U_{p\text{-}f} \cong 12$ eV accounts for the shielding by a 4f electron and $U_{p\text{-}d} \cong 5$ eV for the shielding by the $5d^*$ electron in the final state. Typical examples of L_{III}-edge spectra of metallic and non-metallic Eu^{2+} and Eu^{3+} systems are shown in fig. 2. All L_{III}-edge spectra of RE systems are dominated by strong resonances at energy positions close to the edge. In the early days of XAS, when the spectra were recorded on films, these extreme maxima in the absorption cross section were called "white lines" (WL). They originate from E1 transitions of the 2p electron into empty 5d-states with a high density of states. Figure 2 reveals that the spectral shape of the WL may vary considerably for different systems, for instance for metallic and ionic surroundings. As a general rule, one observes the strongest and sharpest WL in ionic RE^{3+} systems. For this reason, RE trifluorides or sesquioxides are used as reference systems. In metallic systems, the WL is generally broader and less intense. The reasons are simply "solid-state" effects, e.g. interactions of the (mostly empty) 5d-band with ligands and/or with (d)-conduction electrons [15]. For the various divalent or trivalent RE systems, the L_{III}-edge position can vary within $\cong 2$ eV. These chemical shifts reflect the different electronic surroundings (e.g. metallic, ionic) of the RE ions, similar to the variations of the isomer shift within a valence state. We emphasize in this context that these "chemical shifts" act differently on the edge position and on the isomer shift when compared with the impact of different valence states (4f-electron count). This is shown in fig. 3, where the isomer shifts of the Eu systems are plotted versus the respective edge positions. One observes a clear correlation only as long as one compares metallic and non-metallic Eu^{2+} and Eu^{3+} systems.

(b) Valence determination in inhomogeneous mixed-valent rare-earth systems

Because of the easily resolvable energy difference in the edge position for different valence states, L_{III}-edge spectroscopy has been widely applied for valence determination in RE systems and, as will be described in the following, in mixed-

valent systems. Before applying this method to homogeneous mixed-valent systems (intermediate valencies, see refs. [12,16,17]), one has to prove whether the method is capable of determining the *relative* amount of RE^{2+} and RE^{3+} ions in an inhomogeneous mixed-valent systems. A well-suited model system is Eu_3S_4 with Eu^{2+} and Eu^{3+} ions in a ratio of 1:2 on equivalent lattice sites. The near-edge structure of the L_{III}-threshold of Eu_3S_4 (see fig. 1) can be analysed by two thresholds, each consisting of the sum of a Lorentzian (the WL) and an arctan function (the absorption threshold). They are separated by $\cong 7$ eV and exhibit an intensity ratio $r(L_{III})$ near to 1:2, corresponding to a mean valence $v(L_{III}) = 2.63(2)$ and 2.62(3), as determined by two independent studies [7,10].

Such a good agreement with $v = 2.67$, as expected from the stoichiometry of Eu_3S_4, is actually not expected, since there are several reasons or mechanisms which may cause deviations in the observation of an exact one-to-one monitoring of the Eu^{2+} and Eu^{3+} species by their WLs. As explained above, the near-edge structure is the orbital-momentum selected projection of the densities of unoccupied states. The area of the WL is a measure of the number of unoccupied 5d-states. Since the atomic ground-state configurations for RE^{2+} and RE^{3+} are $4f^n5d^06s^2$ and $4f^{n-1}5d^16s^2$, respectively, the WL of an RE^{3+} system may be reduced in its intensity by up to 10% when compared with a corresponding RE^{2+} system. As already mentioned, absorber thickness effects may also strongly influence a correct recording of the near-edge structure. Similar to such effects in Mössbauer spectroscopy, the relative intensity of the dominant resonance line (WL) is reduced with respect to the weaker component [7].

Other reasons for an inequivalent recording of the RE^{2+}/RE^{3+} intensity ratio r by the WLs may originate from solid-state effects, e.g. strong broadenings and/or redistribution of 5d-electron states by hybridization effects with covalent ligands or conduction electrons. These effects are explicitly observable in high-pressure experiments, where the reduced volume enhances hybridization effects, as evidenced by a broadening of the WLs. In some metallic RE^{3+} systems, the WL exhibits a resolved structure due to strong interactions of the 5d states with the (cubic) crystalline-electric field (CEF splitting) [7].

Other effects which may perturb a determination of r in a mixed-valent RE system are (i) final-state effects, and (ii) multiple-scattering processes. In both cases, the near-edge structure, as expected for single-electron transitions into the orbital-momentum selected projection of the density of states, is modified by additional structures. In case (i), the absorption process induces a change in the 4f-electron occupancy of the initial state. In case (ii), the outgoing electron is backscattered via more than one neighbouring atom to the absorbing atom. The possible impact of these effects on a valence determination will be discussed in a following section.

After listing various reasons which may hinder an exact determination of the *absolute* value of r, one should stress that the L_{III}-edge records in a reliable way *relative* changes of r, e.g. as a function of temperature, pressure, and chemical

composition as found in many mixed-valent systems. We will choose examples where the same systems have also been investigated by Mössbauer spectroscopy.

In the past, many intermetallic RE systems with the $ThCr_2Si_2$ structure have been found to exhibit valence instabilities. Two of the best known examples for mixed (or intermediate) valencies are $EuCu_2Si_2$ and $EuPd_2Si_2$, and in both systems ^{151}Eu-Mössbauer spectroscopy has been successfully applied in elucidating their properties [12,18–20]. To study the influence of chemical substitution on the

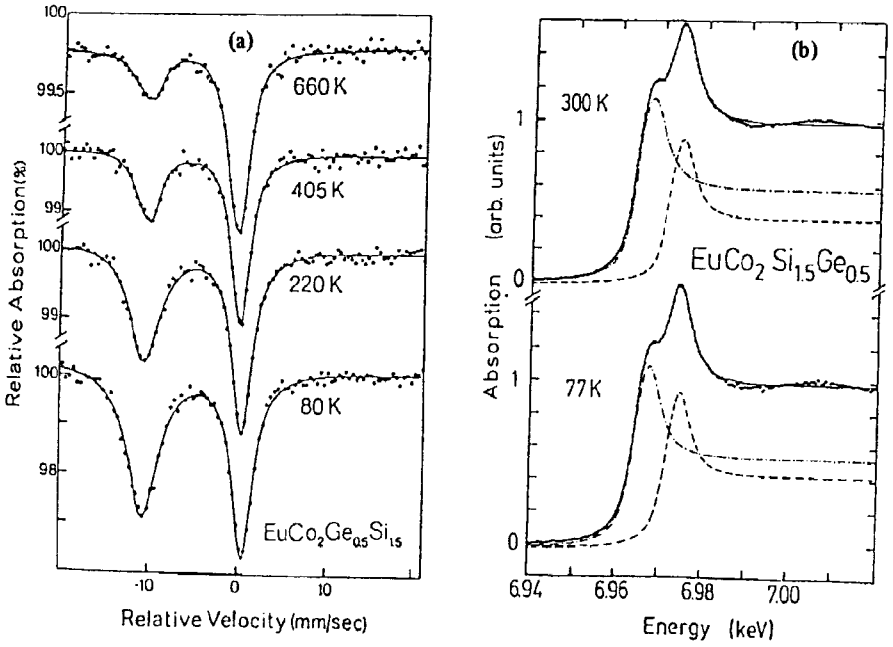

Fig. 4. (a) ^{151}Eu-Mössbauer spectra of inhomogeneously mixed-valent $EuCo_2Si_{1.5}Ge_{0.5}$ at various temperatures [21]. Note the change in the relative intensity of the Eu^{2+} and Eu^{3+} subspectra. (b) Eu-L_{III}-edge spectra of $EuCo_2Si_{1.5}Ge_{0.5}$ at different temperatures.

mixed-valent behaviour of the Eu ions, many quasi-ternary systems of the formula $Eu(Pd_{1-x}M_x)_2Si_2$ or $EuM_2(Si_{1-x}Ge_x)_2$, with M being a d-transition or noble metal, have been investigated. In one of these systems, $EuCo_2(Si_{2-x}Ge_x)_2$, the Eu valence is strongly influenced by the number of Si neighbours. Eu is found to be (almost) trivalent in $EuCo_2Si_2$ and divalent in $EuCo_2Ge_2$. In $EuCo_2Si_{1.5}Ge_{0.5}$, one finds both Eu^{2+} and Eu^{3+} ions [21]. They exhibit a strong temperature dependence on the relative intensity ratio of the well-resolved subspectra (see fig. 4(a)). Careful examination of the same sample by Eu-L_{III}-edge spectroscopy (fig. 4(b)), however, yielded an almost temperature-independent Eu^{2+}/Eu^{3+} ratio. The discrepancy between the two methods could be explained by the measured effective Debye temperatures

of the Eu^{2+} and Eu^{3+} sites, which were found to be considerably different [21]. This example demonstrates that Mössbauer spectroscopy can provide RE^{2+}/RE^{3+} intensity ratios of an inhomogeneous mixed-valent system only after a careful determination of the *f*-factors of the different sites. This holds also for homogeneous mixed-valent systems as long as there are impurity phases present, as often observed [12]. This procedure is, of course, well known in Mössbauer spectroscopy, but has not been applied in most of such studies on mixed-valent systems. The near-edge structure of a stable valent system is not, in contrast to the EXAFS influenced by temperature effects and provides an easy tool for measuring a temperature-independent RE^{2+}/RE^{3+} ratio. In mixed-valent Eu and other RE systems, a temperature-*independent* ratio $r(L_{III})$ can be taken as proof for stable (inhomogeneous mixed-valent) valencies, since homogeneous mixed-valent systems show in general a temperature-dependent ratio $r(L_{III})$, as described by the interconfiguration fluctuation model (ICF model) [12, 18–20,22].

(c) Valence determination in homogeneous mixed-valent systems

The peculiar behaviour of RE ions in a homogeneous mixed-valent state (intermediate valence) has been well characterized by the temperature-dependent isomer shifts, as demonstrated in the case of $EuCu_2Si_2$ and $EuPd_2Si_2$ [18–20]. Intermediate-valent systems can be easily distinguished from inhomogeneous mixed-valent systems by the observation of a single resonance line, since the typical measuring time of the Mössbauer effect is $\cong 10^{-8}$ s, whereas the fluctuation time between the $4f^n$ and $4f^{n-1}5d$ configuration is $\cong 10^{-13}$ s [12,22]. In other RE systems, containing RE ions like Sm, Tm, and Yb ions, the isomer shift is not such a good measure of the valence because of the limited resolution power of the respective Mössbauer transitions [12]. Mixed-valent behaviour or valence changes can, however, be derived from the electric-quadrupole or magnetic-dipole interactions [12].

For intermediate-valent systems, L_{III}-edge spectroscopy is now an often used tool for determining the degree of valence mixing as well as valence transitions induced by temperature, pressure, or chemical compositions. The L_{III}-edge spectra of intermediate-valent RE systems exhibit, as inhomogeneous mixed-valent systems, the $4f^n$ and $4f^{n-1}$ subspectra, since the measuring time of the edge spectroscopy is determined by the lifetime of the 2p hole ($\cong 10^{-15}$ s), which is shorter than the fluctuation time of the 4f configurations. Typical applications of L_{III}-edge spectroscopy are the studies of SmS (as a function of chemical composition [23]), of TmSe [24] and of Yb metal (as a function of pressure [25]).

The pressure-induced valence transition in SmS, as studied by L_{III}-edge spectroscopy [10,26], is shown in fig. 5. The L_{III}-edge spectra monitor the valence transition, which occurs within a narrow pressure range at $\cong 6.5$ kbar, by a dramatic change of their spectral shape. Figure 6 displays the pressure dependence of the Sm^{3+} subspectrum together with the Sm-S distance, which was derived from the analysis of

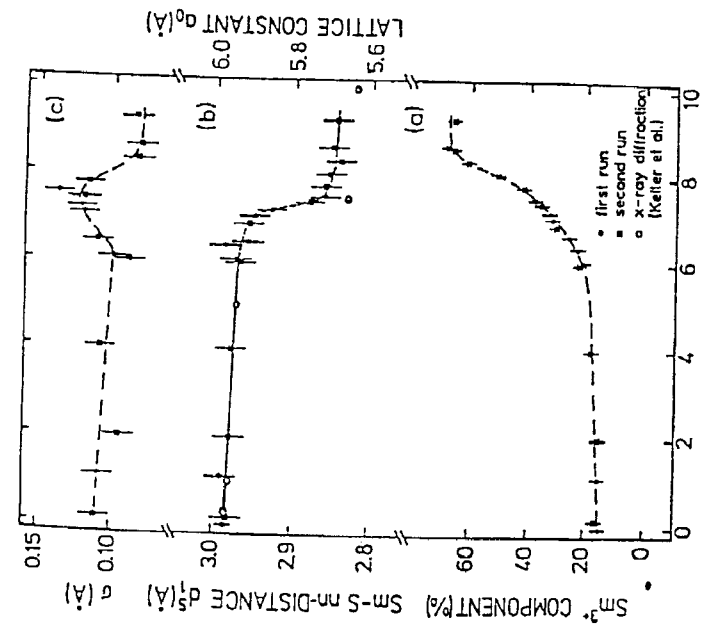

Fig. 6. (a) Pressure dependence of the relative intensity of the Sm^{3+} subspectra in SmS (see fig. 5). (b) Sm-S distance in SmS as determined by Sm-L_{III} EXAFS (full squares and dots) and by X-ray diffraction (open dots). (c) Mean-squared displacements σ of the Sm-S distance from the EXAFS analysis (from refs. [10,26,27]).

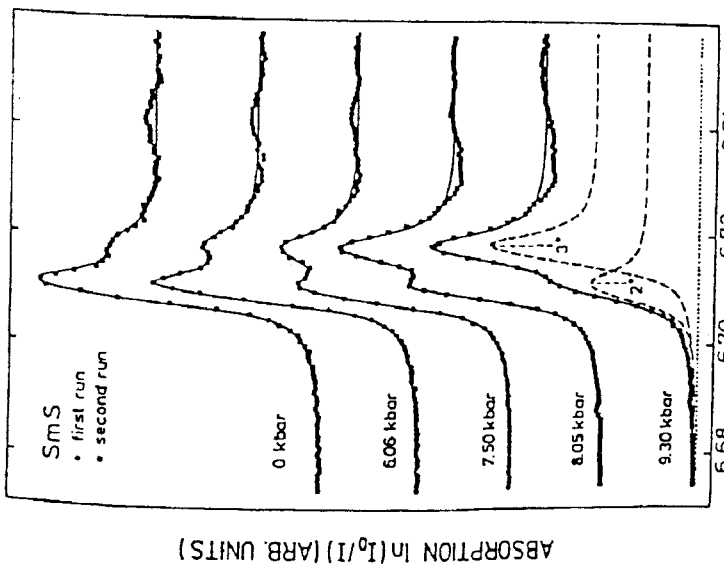

Fig. 5. Sm-L_{III}-edge spectra of SmS as a function of hydrostatic pressure [10,26].

the EXAFS measured in the same L_{III}-spectra. A closer inspection of fig. 6 indicates that the near-edge spectra monitor the onset of the valence transition at lower pressures than the lattice constant. The occurrence of a 15% Sm^{3+} component already at ambient pressure is, as shown by an L_{III}-edge study of single-crystals of $Sm_{1-x}Y_xS$ in fluorescence mode, due to impurities and defects introduced by the grinding of SmS used in the pressure study [27].

Of special interest for this review are comparative studies of mixed-valent systems by L_{III}-edge spectroscopy and Mössbauer effect. In such studies, we used identical samples for both methods, contained even in the same sample holders. Such procedure is, in our opinion, mandatory in comparative studies, since these systems may exhibit differences in their mixed-valent behaviour, even when different pieces of the same batch are used. The reasons for such differences are site disorder caused, for instance, by an occupation of the Pd site by Si or vice versa, and impurity phases (satellite lines in the Mössbauer spectra), which are present to some extent in most of the mixed-valent systems with the $ThCr_2Si_2$ structure [12].

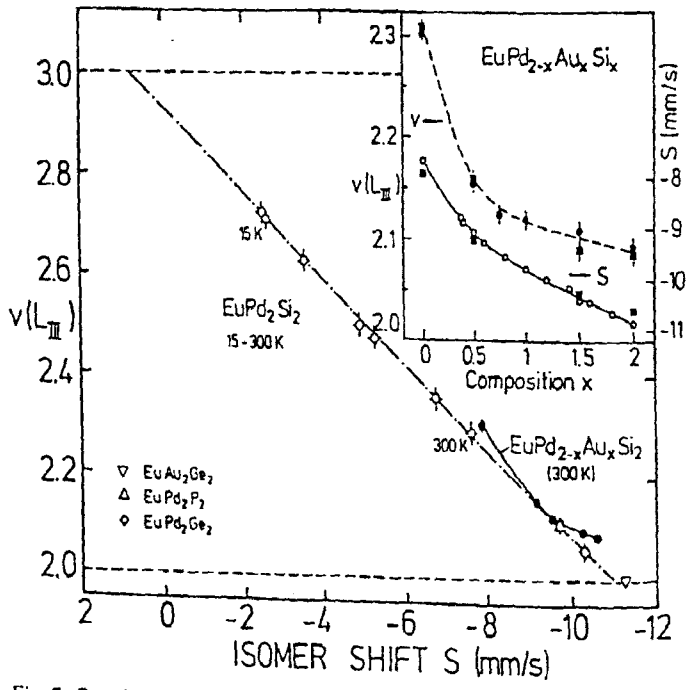

Fig. 7. Correlation between the averaged ^{151}Eu isomer shift S and $v(L_{III})$ for the temperature-induced valence transition in $EuPd_2Si_2$ (open dots), $EuPd_{2-x}Au_xSi_2$ (full dots) and related systems [28,31,33]. The inset shows the explicit dependence of S and $v(L_{III})$ on the Au substitution.

In a comparative L_{III}-edge and Mössbauer study of the temperature-induced valence transition in $EuPd_2Si_2$ we derived, as shown in fig. 7, an almost linear corre-

lation between $v(L_{III})$ and the isomer shift S [28]. From this it was concluded that both methods monitor in a reliable way the *relative* valence change in this system. A similar comparative study of $EuPd_2Si_2$ by Kemly et al. [29] arrived at the same conclusion, but stressed the point of an *absolute* determination of the valency by $v(L_{III})$. Neither of the studies [28,29] found the strong non-linearities in the $v(L_{III})$/isomer shift correlation that were claimed by Röhler in a previous study of $EuPd_2Si_2$ and $EuCu_2Si_2$ [30].

We extended the comparative studies to the $EuPd_{2-x}Au_xSi_2$ series [31]. This system is of special interest since it is considered as one of the few examples for the transition from a mixed-valent to a magnetic-ordering behaviour [32–34]. In particular, it was claimed that at $x = 0.36$, where the onset of magnetic ordering is observed, the Eu ions are still mixed-valent, with an average valence of $\cong 2.2$ [32]. Figure 8 shows typical L_{III}-edge spectra of $EuPd_{2-x}Au_xSi_2$ and, for comparison, a spectrum of $EuAu_2Ge_2$. Interestingly, all L_{III}-edge spectra of the $EuPd_{2-x}Au_xSi_2$ series exhibit a double-peaked edge structure, even $EuAu_2Si_2$, where a "valency" $v(L_{III}) = 2.09$ was derived. On the other hand, Mössbauer studies of $EuPd_{2-x}Au_xSi_2$ show, for $x \geqslant 0.5$, a behaviour typical for divalent Eu, i.e. no temperature variation of the isomer shifts. $EuAu_2Si_2$ retains its divalent character even under pressures up to 30 kbar [34]. Only $EuAu_2Ge_2$ is found to be divalent from the L_{III}-edge; its isomer shift ($S = 11.2$ mm/s) is an extreme negative value for a metallic Eu^{2+} system. Both the $v(L_{III})$ and S values of $EuAu_2Ge_2$ fit well as pure Eu^{2+} endpoint in the $v(L_{III})/S$ correlation of $EuPd_2Si_2$ (fig. 7).

The reasons why Eu in the $EuPd_{2-x}Au_xSi_2$ for $x \geqslant 0.5$ series is not divalent, as suggested from a careful Mössbauer study [33], but apparently mixed-valent from the L_{III}-edge will be outlined in the following sections, where even more extreme examples of discrepancies between $v(L_{III})$ values and valencies derived from other methods will be given. It should be pointed out that in the $EuPd_{2-x}Au_xSi_2$ series, $v(L_{III})$ and S vary in a different way with the Au substitution x (see inset of fig. 7), which leads to non-linearity in the $v(L_{III})/S$ diagram at $x = 0.5$ (fig. 7) where the transition from intermediate-valent behaviour to stable valencies occurs [31–33].

One should mention at this point another deviation in the L_{III}-edgee spectra of the $EuPd_{2-x}Au_xSi_2$ series from a "normal" mixed-valent behaviour. The energy separation between the Eu^{2+} and Eu^{3+} thresholds ΔE is not constant but depends on the average valence of the Eu ions. The reason for this behaviour is attributed to the change in the valence-band d-electron occupancy, which changes as a function of the average Eu valency [30]. This dependence was found to be roughly linear with $v(L_{III})$ for the temperature-induced valence change in $EuPd_2Si_2$. In $EuPd_{2-x}Au_xSi_2$, however, ΔE deviates strongly from this linear relation for $x \geqslant 0.5$, as shown in fig. 9, indicating a change in the mixed-valent behaviour of the Eu ions [31].

In $EuPd_2Si_2$, the temperature-induced change in valency as derived by ME and $v(L_{III})$ is $\cong 0.43$ between 15 K and 300 K [28]. Here, we briefly present the results of a recent comparative study of another Eu system, where the overall valence change in

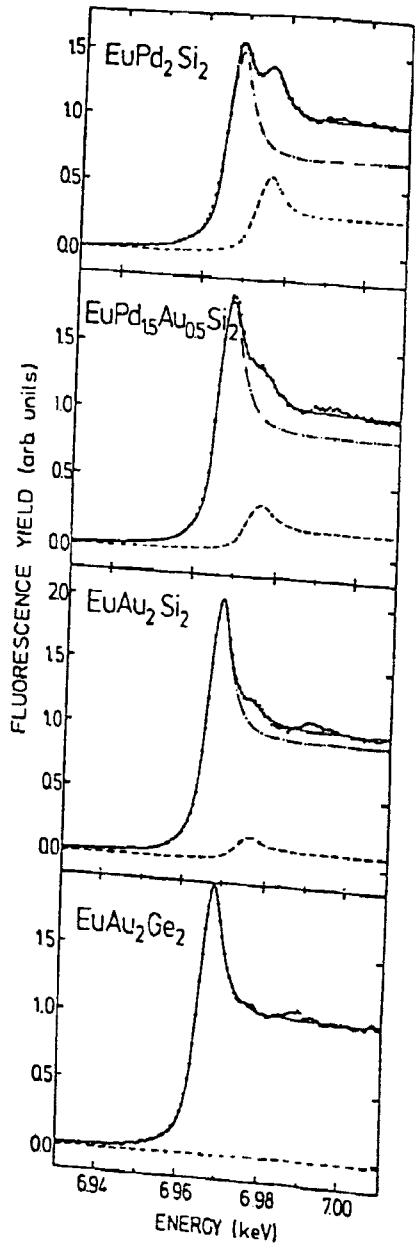

Fig. 8. Eu-L_{III}-edge spectra of $EuPd_{2-x}Au_xSi_2$ and $EuAu_2Ge_2$ [31].

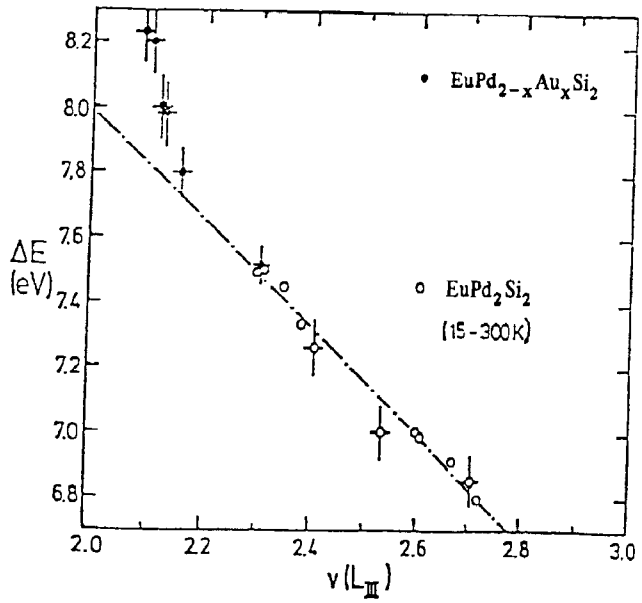

Fig. 9. Plot of the energy separation ΔE between the Eu^{2+} and Eu^{3+} subspectra of the Eu L_{III}-edge in $EuPd_2Si_2$ and $EuPd_{2-x}Au_xSi_2$ [31] as a function of $v(L_{III})$.

the same temperature region is even larger. In the $EuNi_2Si_{2-x}Ge_x$ system, we found for $x = 1.5$ intermediate valencies of the different Eu sites, with an overall temperature-induced valence change of $\cong 0.55$ [35]. Following the concept outlined previously for the substituted mixed-valent system $La_{1-x}Eu_xRh_2$ [36] and also applied to the $EuPd_{2-x}Au_xSi_2$ system [33,34], we attributed to each Eu site, according to the number of nearest Si/Ge neighbours, a different mixed-valent behaviour. This is demonstrated in the analysis of the ^{151}Eu-Mössbauer spectra of $EuNi_2Si_{0.5}Ge_{1.5}$ shown in fig. 10. Typical L_{III}-edge spectra of $EuNi_2Si_{0.5}Ge_{1.5}$ are shown in fig. 11, together with the reference systems $EuNi_2Si_2$ and $EuNi_2Ge_2$. The plot of the averaged values of S versus $v(L_{III})$ for $EuNi_2Si_{0.5}Ge_{1.5}$ is shown in fig. 12, together with the corresponding values for $EuNi_2Ge_2$ and $EuNi_2Si_2$. The dashed-dotted curve, connecting the points derived from S values as obtained from the areas of the various subspectra, exhibit a slight deviation from a linear correlation. Using the concept developed in the $EuCo_2Si_{2-x}Ge_x$ system, we measured the effective Debye temperatures for $EuNi_2Si_2$ and $EuNi_2Ge_2$ and corrected the spectral areas of the various sites by linear extrapolation according to the number of Si/Ge neighbours. The corrected values of S_{corr} yield a linear correlation with $v(L_{III})$. $EuNi_2Si_2$, near to trivalency from $v(L_{III})$ and the temperature-dependent isomer shift, fits excellently in this correlation. On the other hand, it is surprising that $EuNi_2Ge_2$ is "mixed-valent" from the L_{III}-edge, $v(L_{III}) = 2.15$, but normal divalent from isomer shift (no temperature

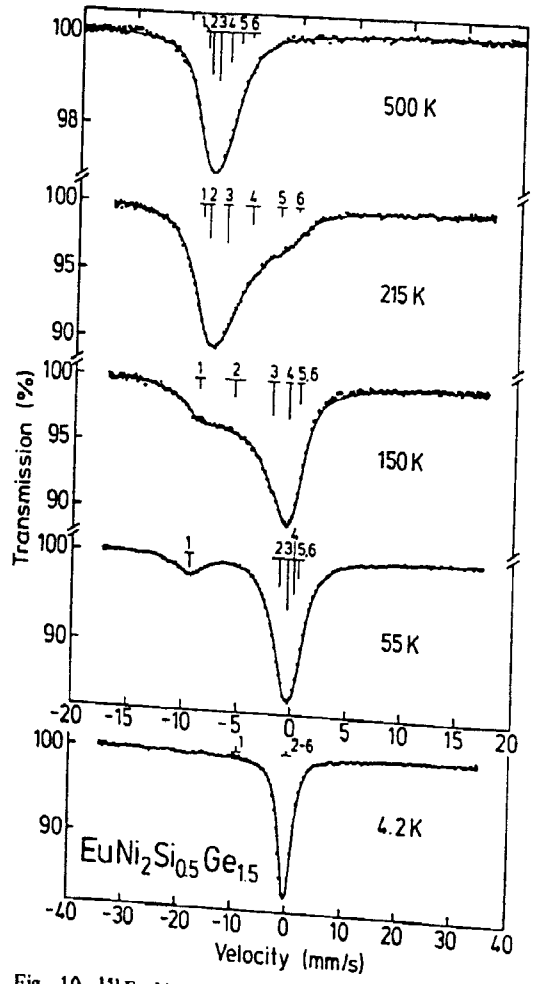

Fig. 10. ^{151}Eu-Mössbauer spectra of $EuNi_2Si_{0.5}Ge_{1.5}$ at various temperatures. The bars indicate the intensity and width of the subsepctra.

dependence), magnetic hyperfine field and magnetic ordering temperature [37]. As in the case of $EuAu_2Si_2$, we attribute this behaviour to a final-state effect intimately connected with the L_{III}-edge spectroscopy (see next section).

From the comparative studies of the $EuPd_{2-x}Au_xSi_2$ and the $EuNi_2Si_{2-x}Ge_x$ systems, we conclude that both methods, when carefully applied, monitor the relative change in valency in a linear way. Absolute values in valency as determined by L_{III}-edge spectroscopy may deviate by 0.15. This is especially the case for divalent or nearly divalent systems, where covalent effects may introduce a change in 4f-occupancy by the absorption process. One should also comment on trivalent RE impurities affecting

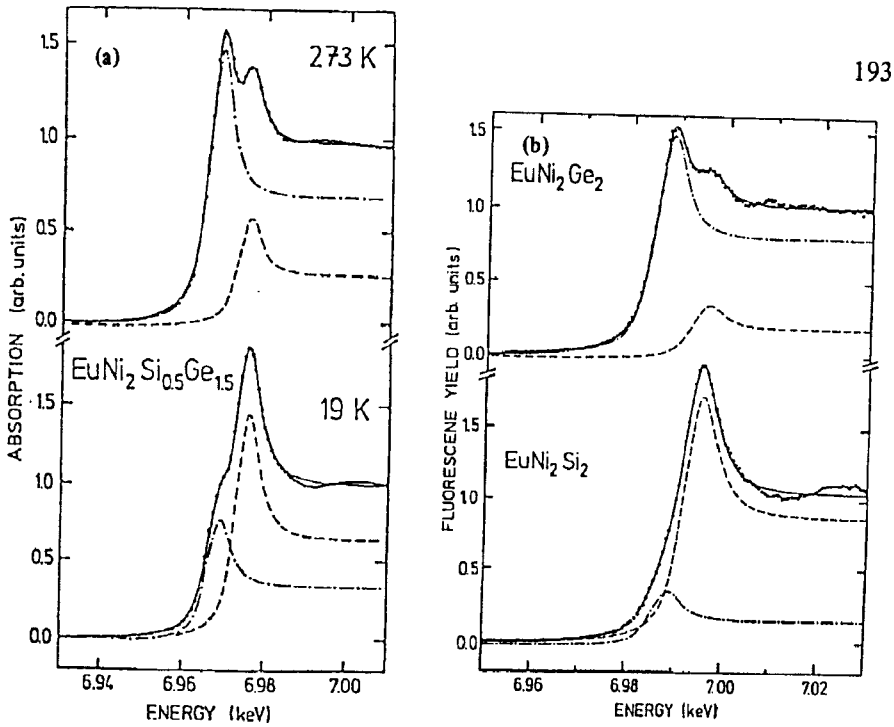

Fig. 11. Eu-L_{III}-edge spectra of (a) $EuNi_2Si_{0.5}Ge_{1.5}$ at various temperatures and of (b) the references systems $EuNi_2Si_2$ and $EuNi_2Ge_2$.

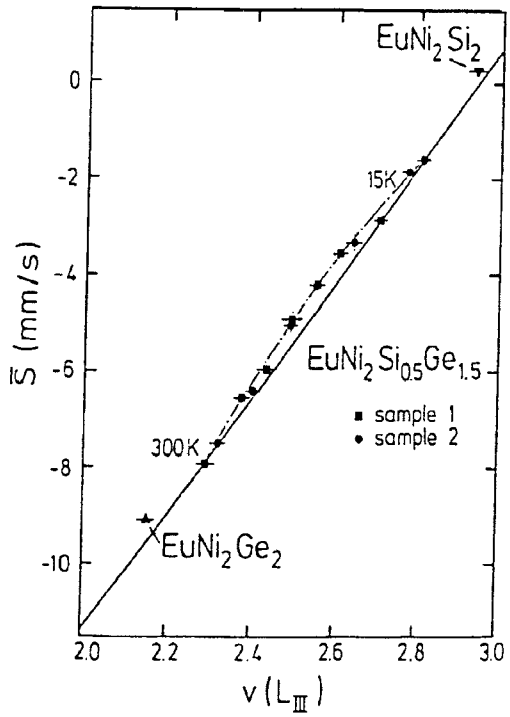

Fig. 12. Correlation between the averaged isomer shifts S and $v(L_{III})$ in $EuNi_2Si_{0.5}Ge_{1.5}$. The solid dots and squares are obtained when S is not corrected for different S factors of the subspectra. A correction of S results in a linear correlation, as indicated by the straight line.

the L_{III}-edge spectra of divalent RE systems. In the case of EuM_2X_2 systems, such impurity phases are detectable in the Mössbauer spectra with an accuracy of $\cong 1\%$ of the total spectral intensity. We have devoted a special study to this problem [38]. When correcting the $v(L_{III})$ values for such contaminations, one has to consider that typical Eu^{3+} impurity phases (e.g. Eu_2O_3, which can be characterized by its isomer shift) exhibit a larger WL intensity than Eu in metallic systems (see fig. 2).

(d) Final-state effects in L_{III}-edge spectroscopy

In this review on L_{III}-edge spectroscopy, we are already confronted with the fact that two normal divalent systems ($EuAu_2Si_2$ and $EuNi_2Ge_2$) exhibit double-peaked edge structures, from which one could claim "mixed-valent" properties. Also in $EuCo_2Si_2$ one finds $v(L_{III}) = 2.15$, in contrast to the divalency proved by the magnetic properties and the Mössbauer parameters (stable divalent even under pressures up to 60 kbar [21,39]. Such discrepancies were first detected in a closely related system, $EuPd_2P_2$, where Mössbauer effect and magnetic studies proved the divalency of Eu, but the L_{III}-edge yielded $v(L_{III}) = 2.13(2)$ [40–42]. The observed trivalent component in the L_{III}-edge spectrum was attributed to a final-state effect, which means a change of the $4f^7$ configuration of the ground state by the promotion of a 4f-electron into a ligand bond (analogous to a shake-up process in 3d-XPS) [40]. Multiple scattering effects as the reason for the peak at the Eu^{3+} position in the $EuPd_2P_2$ L_{III}-edge spectrum were excluded, since in isostructural reference systems (e.g. $GdPd_2P_2$) such features are absent. In the dilute system $Eu_{0.05}Y_{0.95}Pd_2P_2$, the L_{III}-edge spectrum also exhibited a double-peaked structure, from which $v(L_{III}) = 2.10(3)$ was derived (after correction for a small Eu_2O_3 impurities phase) [38]. This observation supported the assumption that final-state effects are caused by covalent Eu-ligand interactions, and not by Eu-Eu interactions [42]. Other deep-core spectroscopies, like 3d-XPS, also observe final-state effects in $EuPd_2P_2$, in contrast to a shallow level spectroscopy like valence-band photoemission, where the divalent nature of Eu in $EuPd_2P_2$ was confirmed [43].

To summarize the studies of divalent EuM_2X_2 systems, with M = Pd, Au, Co, Ni and X = P, Si, Ge, we mention that a purely "divalent" L_{III}-edge spectrum as observed in $EuAu_2Ge_2$ is the exception. In the other systems, where the divalency of the Eu ions is confirmed by other methods, we find $v(L_{III})$ values deviating from 2 (see table 1). When comparing in these systems the values of the isomer shift, the magnetic hyperfine field and ordering temperature with $v(L_{III})$, one observes a rough correlation similar to that found more explicitly in the $EuPd_{2-x}Au_xSi_2$ series (fig. 7). Systems with $v(L_{III}) \cong 2.15$ are near to the border of intermediate valencies, as demonstrated strikingly by the high-pressure studies of $EuPd_{1.6}Au_{0.4}Si_2$ [34]. We hesitate, however, to call systems "weakly" mixed-valent [34] as long as experimental evidence for this behaviour is only drawn from the L_{III}-edge or other deep-core spectroscopies. In Eu systems, the Mössbauer effect provides by the isomer shift and

Table 1

Compilation of Mössbauer data and $v(L_{III})$ values for Eu systems with $ThCr_2Si_2$ structure. The isomer shifts S are given at 300 K, the magnetic hyperfine fields B_{eff} at 4.2 K. The values of S and B_{eff} are given with an accuracy of ± 0.05 mm/s and ± 5 kG, respectively. For details, see the references

System	S (mm/s)	B_{eff} (kG)	T_N (K)	$v(L_{III})$	Ref.
$EuNi_2Ge_2$	− 9.1	400	30	2.15(3)	[35,37]
$EuCo_2Ge_2$	− 9.5	370	23	2.15(5)	[35,37,39]
$EuPd_2P_2$	− 9.7	360	30	2.13(2)	[38,40–42]
$Eu_{0.05}Y_{0.95}Pd_2P_2$	− 10.4	n.m.	n.m.	2.10(2)	[38]
$EuAu_2Si_2$	− 10.4	340	6.5	2.09(2)	[31,33,34]
$EuPd_2Ge_2$	− 10.3	310	16	2.05(2)	[38]
$EuAu_2Ge_2$	− 11.2	n.m.	n.m.	2.00(1)	[31]

its characteristic variation on temperature and pressure an extremely sensitive tool for a characterization of an intermediate valency. A true valency of ≅2.2, together with a reasonable estimate of E_{mix}, leads to a pronounced variation of S with temperature and/or pressure as observed, for instance, in the $EuPd_{1-x}Au_xSi_2$ system for pressures above ≅6 kbar (x = 0.4) and ≅30 kbar (x = 0.6), respectively, where the magnetism suddenly disappears [34]. The interesting properties of a metallic system on the verge of intermediate valency, e.g. the increase in magnetic ordering temperature, can be explained by an increased hybridization of the RE ion, including even the 4f-electrons [40]. The peculiar properties of the 4f-electrons in an insulating system ($TmSe_{1-x}Te_x$) near to a valence transition are described in ref. [44] as "slightly delocalized", which seems to be equivalent to a hybridization.

We want to mention at this point L_{III}-edge and Mössbauer studies, performed in other laboratories, of two important Eu systems, namely EuO and Eu metal, where also pronounced discrepancies in valencies, as determined by the two spectroscopies, are evident. A high-pressure L_{III}-edge study of EuO observes a transition to mixed-valent behaviour (that means a double-peaked absorption edge) already at pressures as low as ≅60 kbar [45]. At 150 kbar, the L_{III}-edge spectra reveal $v(L_{III}) \cong 2.2$, when corrected for the Eu_2O_3 impurity phase. On the other hand, Mössbauer studies of EuO up to 150 kbar do not find experimental evidence for mixed-valent behaviour [46]. An extension of this study to pressures up to 300 kbar by the use of a diamond-anvil cell is reported by Taylor [47]. At 300 kbar, a drop in the magnetic ordering temperature gives strong evidence for the onset of an intermediate valence in EuO. Both Mössbauer studies are in conflict with a high-pressure study of the lattice constant

and the semiconducting gap, observing indications of a valence transition around 120 kbar [48]. In Eu metal, double-peaked structures of the L_{III}-edge are developing rapidly under pressure already at 50 kbar, and a value $v(L_{III}) = 2.5$ was derived at 120 kbar [49]. A recent Mössbauer study of Eu metal found up to 120 kbar a strong, but linear variation of the isomer shift and still magnetic order [49], which seems to be in contrast to the valency derived from the L_{III}-edge [32]. In both EuO and Eu metal, the question of whether there is a coexistence of magnetic order and intermediate valencies is, in our opinion, still controversial from the results of two spectroscopies and requires additional high-pressure studies.

In analogy with the above outlined arguments on final-state effects in EuM_2X_2 systems, we want to stress the point that the observation of a double-peaked L_{III}-edge structure is not a proof of the mixed valency in the investigated systems. Valence transitions in Eu systems can be proved by the observation of a temperature-dependent variation of the Eu^{2+}/Eu^{3+} ratio, as evidenced, for instance, by a strong temperature dependence of the isomer shift. Double-peaked L_{III}-edge spectra, on the other hand, may be indicative of strong covalent effects, involving even the 4f-electrons. A mixed-valent system in the definition as given, for instance, in ref. [51], demands that, in the case of Eu, the $4f^6$ level is pinned at the Fermi level. In insulating systems, a transition to an intermediate valence, with SmS as best example, is accompanied by an insulator/metal transition. In metallic systems, valence transitions are monitored by the characteristic changes in a variety of other properties, e.g. the lattice constant, the magnetic susceptibility and the magnetic ordering behaviour. One should mention the $Yb_{1-x}In_xCu_2$ system as a new textbook example of a valence transition in a metallic system, which was studied recently by a variety of methods, including L_{III}-edge and Mössbauer spectroscopy [52].

Final-state effects in L_{III}-edge spectroscopy are expected to be even more pronounced in Ce systems because of the less-localized character of the 4f-electrons, which results in a wide variety of transport properties of metallic Ce systems. L_{III}-edge spectroscopy has often been applied for the investigation of their properties [53,54], with a still ongoing discussion in terms of mixed valency or hybridization effects [54]. Final-state effects are even more pronounced in the L_{III}-edge spectra of insulating, formally tetravalent systems like CeO_2 and CeF_4 (as in the Pr and Tb homologs). In these systems, the L_{III}-edge exhibits additional structures which can only be explained by multi-electron transitions [55–57]. It should be mentioned that the complex 3d-XPS as well as the L_{III}-edge spectra are now well-described by the same theoretical treatment [58]. Because of space limitations, we will review neither these systems nor the $M_{IV,V}$-edge spectroscopy, which has been applied successfully to their investigation [57,59].

We do, however, wish to briefly report on L_{III}-edge studies where the *polarization* dependence of the absorption process was used to demonstrate that the final-state effects in covalent systems may depend on the direction of the covalent bonds. We investigated a single crystal of CeNi in fluorescence mode with the E vector of the

linear-polarized synchrotron radiation at different angles with respect to the crystallographic axes. CeNi has an orthorhombic structure and exhibits anomalies in the temperature dependence of the lattice constants (increase of the *b*-axis with decreasing temperature) and of the magnetic susceptibility (loss of magnetic moment), which are attributed to (anisotropic) covalent Ce-Ni bonds [60]. The double-peaked L_{III}-edge spectra of the CeNi single crystal exhibit differences in the relative weights of the (formal) $Ce^{3+}(4f^1)$ and $Ce^{4+}(4f^0)$ subspectra as functions of temperature *and* orientation [61]. The Ce^{4+} component is strongest when the *E* vector is parallel to the direction of the shortest Ce-Ni bond. For this reason, we consider the value of $\upsilon(L_{III})$ as a measure of the (anisotropic) f-d hybridization, but not as a measure of the Ce valence [61].

In this context, one should mention Cu L_{III}-edge absorption studied performed on the new high-T_c superconductors, where the valencies of the Cu ions are of actual interest. Using single crystalline [62] or highly textured samples [63] of $YBa_2Cu_3O_{7-\delta}$, it could be demonstrated that a satellite in the Cu-L_{III} absorption spectra, which has been attributed to Cu^{3+} ions and which is strongest for probes with the highest T_c, changes its relative intensity with the orientation of the sample. The largest satellite is observed when the polarization vector of the synchrotron radiation is parallel to the crystallographic *c*-axis of $YBa_2Cu_3O_{7-\delta}$ [62,63]. These observations are interpreted as direct experimental evidence for itinerant holes at the oxygen ligands, which are responsible for the superconducting properties of these systems.

The new superconductors of $YBa_2Cu_3O_{7-\delta}$ type have also been investigated at the Cu K-edge. Since there are two different Cu sites, the interpretation of the complex edge spectra was rather controversial. Recent studies showed that the choice of appropriate reference systems (with similar oxygen configurations) *and* of oriented samples, together with polarized synchrotron radiation, enables a reliable interpretation of the K-edge spectra [64,65].

3.2. BOND LENGTH AND ORIENTATION IN MOLECULAR SYSTEMS FROM EDGE SPECTROSCOPY

XAS has been very successfully applied to study the orientation and bond length of molecules adsorbed on surfaces [8,66]. In simple, low-*Z* molecules like C_2H_6, C_2H_4, and C_2H_2, one observes strong resonances in the near-edge region of the C-K thresholds, which can be attributed to electron transitions into π^* and σ^* orbitals. From a systematic investigation of the near-edge structure of such molecules in gaseous form, Stöhr et al. [67,68] found a linear correlation between the energy position of the σ^* resonance and the intramolecular bond length. This scheme has been applied to determine the modified bond length of these molecules when adsorbed on surfaces [68]. This application of edge spectroscopy (NEXAFS) is particularly

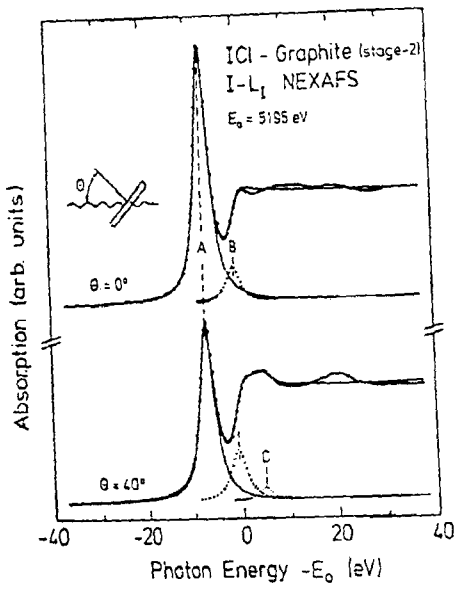

Fig. 13. Iodine L_I-edge spectra of ICl graphite at various orientations with respect to the polarization of the synchrotron radiation [70].

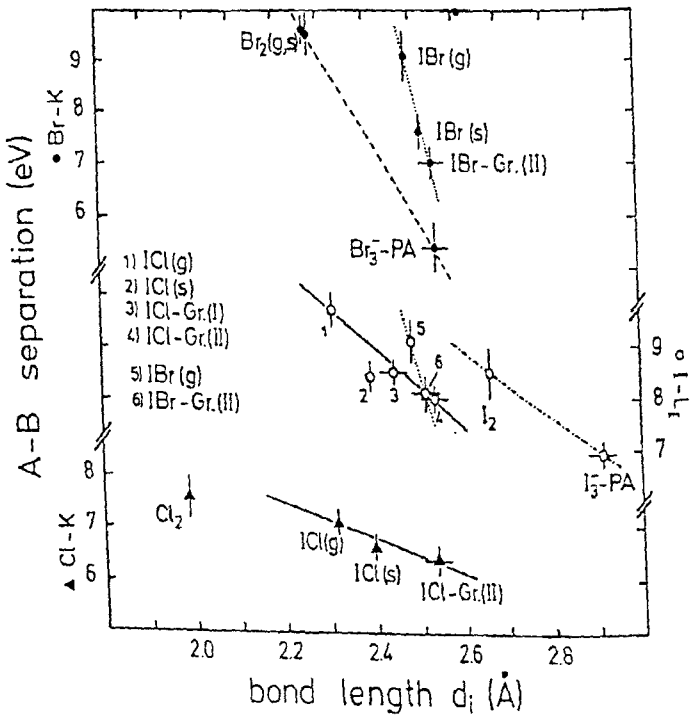

Fig. 14. Correlation between the energy separation of the σ^* resonance (peak A) and the edge (peak B) of various halogen molecules and polyanions [71].

useful for such dilute systems when compared with EXAFS spectroscopy, which is normally used for bond length determinations.

We have performed similar NEXAFS and EXAFS studies of halogen molecules and polyanions (e.g. I_2, Br_2, Cl_2, ICl, IBr, I_3^-, Br_3^-) in gaseous and solid form as well as intercalated in graphite or polyacetylene [69–71]. The pre-edge region of the respective Cl-K, I-L_1, and Br-K thresholds is dominated by strong σ^* resonances, which sensitively monitor the orientation of the molecules, as shown in the I-L_1 spectra of ICl graphite (fig. 13). For the various halogen molecules, we also derived a correlation between the position of the σ^* resonance with respect to the edge and the intramolecular bond lengths, which is shown in fig. 14. For complementary studies of these systems, the ^{129}I-Mössbauer resonance is particularly useful, as demonstrated in ref. [72].

3.3. INVESTIGATION OF SPIN-DENSITIES IN MAGNETIC SYSTEMS BY NEXAFS WITH CIRCULARLY-POLARIZED SYNCHROTRON RADIATION

A new and fascinating application of XAS was recently introduced by Schütz et al. [9]. Using the spin-dependent absorption of circularly-polarized synchrotron radiation, the spin-polarization of the unoccupied p- and d-band states of ferromagnetic Fe [9] as well as Gd and Tb metal [73] was studied. The method allows an elegant mapping of the spin densities of the p- and d-states up to $\cong 50$ eV above the Fermi level and offers a promising tool for the study of magnetic phenomena like critical fluctuations and magnetic excitations. Another related application is the measurement of magnetic EXAFS [74]. Magnetic studies with XAS will certainly be a rapidly expanding field in the near future.

Acknowledgements

The author wants to thank J. Feldhaus, K.H. Frank, G. Kalkowski, W. Krone, B. Perscheid, T. Schedel, G. Schmiester, E.V. Sampathkumaran, I. Nowik, and G. Kaindl for fruitful cooperation during the course of the investigations presented here. This work was supported by the BMFT, Grant No. 05 313AXB/TP4 and, in part, by the Sfb-337, TP B2.

References

[1] *Synchrotron Radiation Research* ed. H. Winick and S. Doniach (Plenum Press, New York, 1980) Ch. 10, 12 and 13.
[2] *Handbook on Synchrotron Radiation*, ed. E.E. Koch (North-Holland, Amsterdam, 1983).
[3] *X-Ray Absorption*, ed. D.C. Koningsberger and R. Prins (Wiley, New York, 1988).
[4] *EXAFS and Near Edge Structure III*, ed. K.O. Hodgson, B. Hedman and J.E. Penner-Hahn (Springer Proceedings in Physics 2, Berlin, 1984).

[5] *EXAFS and Near Edge Structure IV*, ed. P. Lagarde, D. Raoux and J. Petiau, J. de Phys. 47, Colloq. C8, Suppl. 12 (1986).
[6] *Proc. of the XAFS-V Conf.* (Seattle, 1988), to appear in Physica B.
[7] For a recent review of edge spectroscopy on rare-earth systems, see J. Röhler, in: *Handbook on the Physics and Chemistry of Rare Earths*, Vol. 10, ed. K.A. Gschneidner, Jr., L. Eyring and S. Hüfner (Elsevier, Amsterdam, 1987) p. 453.
[8] D. Norman, J. Phys. C19(1986)3273.
[9] G. Schütz, W. Wagner, W. Wilhelm, P. Kienle, R. Zeller, R. Frahm and G. Materlik, Phys. Rev. Lett. 548(1987)737.
[10] K.H. Frank, Ph.D. Thesis, Freie Universität Berlin (1984).
[11] See, for example, C.R. Natoli and M. Benfatto, in ref. [5], p. C8-11; M. Benfatto et al., ibid. p. C8-25.
[12] I. Nowik, Hyp. Int. 13(1983)89.
[13] E.R. Bauminger, G.M. Kalvius and I. Nowik, in: *Mössbauer Isomer Shifts*, ed. G.K. Shenoy and F.E. Wagner (North-Holland, Amsterdam, 1978) p. 661.
[14] J. Feldhaus, Ph.D. Thesis, Freie Universität Berlin (1982).
[15] G. Materlik, B. Sonntag and M. Tausch, Phys. Rev. Lett. 51(1983)267; G. Materlik, J.E. Müller and J.W. Wilkins, Phys. Rev. Lett. 50(1983)267.
[16] *Valence Instabilities*, ed. P. Wachter and J. Boppart (North-Holland, Amsterdam, 1982).
[17] *Proc. Int. Conf. on Valence Fluctuations*, J. Magn. Magn. Mater. 47 & 48(1985).
[18] E.R. Bauminger, D. Froindlich, I. Nowik, S. Ofer, I. Felner and I. Mayer, Phys. Rev. Lett. 30(1973)1053.
[19] J. Röhler, D. Wohlleben, G. Kaindl and H. Balster, Phys. Rev. Lett. 49(1982)65.
[20] E.V. Sampathkumaran, L.C. Gupta, R. Vijayaraghavan, K.V. Gopalakrishnan, R.G. Pillay and H.G. Devare, J. Phys. C14(1981)L237.
[21] B. Perscheid, I. Nowik, G. Wortmann, G. Schmiester, G. Kaindl and I. Felner, Z. Phys. B 73(1989)511.
[22] D. Wohlleben, in: *Valence Fluctuations in Solids*, ed. L.M. Falicov, W. Hanke and M.P. Maple (North-Holland, Amsterdam, 1981) p. 1.
[23] M. Martin, J.B. Boyce, J.W. Allen and F. Holtzberg, Phys. Rev. Lett. 44(1980)1275.
[24] H. Launois, M. Rawiso, E. Holland-Moritz, R. Pott and D. Wohlleben, Phys. Rev. Lett. 44(1980)1271.
[25] K. Syassen, G. Wortmann, J. Feldhaus, K.H. Frank and G. Kaindl, Phys. Rev. B26(1982) 4775.
[26] K.H. Frank, G. Kaindl, J. Feldhaus, G. Wortmann, W. Krone, G. Materlik and H. Bach, in ref. [16], p. 189.
[27] K.H. Frank et al., to be published.
[28] G. Wortmann, K.H. Frank, E.V. Sampathkumaran, B. Perscheid, G. Schmiester and G. Kaindl, J. Magn. Magn. Mater. 49(1985)325.
[29] E. Kemly, M. Croft, V. Murgai, L.C. Gupta, C. Godart, R.D. Parks and C.U. Segre, J. Magn. Magn. Mater. 47 & 48(1985).
[30] J. Röhler, J. Magn. Magn. Mater. 47 & 48(1985)175.
[31] G. Wortmann, W. Krone and B. Perscheid, J. de Phys. 47(1986)C8-979.
[32] C.U. Segre, M. Croft, J.A. Hodges, V. Murgai, L.C. Gupta and R.D. Parks, Phys. Rev. Lett. 49(1982)1947.
[33] M.M. Abd-Elmeguid, Ch. Sauer, K. Köbler and W. Zinn, Z. Phys. B60(1983)239.
[34] M.M. Abd-Elmeguid, Ch. Sauer and W. Zinn, Phys. Rev. Lett. 55(1985)2467.
[35] G. Wortmann, B. Perscheid, I. Nowik, G. Kaindl and I. Felner, to be published.
[36] E. Bauminger, I. Felner, D. Levron, I. Nowik and S. Ofer, Phys. Rev. Lett. 33(1974)890; E. Bauminger et al., J. de Phys. C6(1979)61.

[37] I. Felner and I. Nowik, J. Phys. Chem. Solids 39(1978)767.
[38] G. Wortmann, W. Krone, E.V. Sampathkumaran and G. Kaindl, Hyp. Int. 28(1986)581.
[39] G. Wortmann, unpublished results.
[40] E.V. Sampathkumaran, G. Kaindl, W. Krone, B. Perscheid and R. Vijayaraghavan, Phys. Rev. Lett. 54(1985)1067.
[41] E.V. Sampathkumaran, B. Perscheid, W. Krone and G. Kaindl, J. Magn. Magn. Mater. 47&48(1985)410.
[42] E.V. Sampathkumaran, B. Perscheid and G. Kaindl, Solid State Commun. 51(1984)701.
[43] G.K. Wertheim, E.V. Sampathkumaran, C. Laubschat and G. Kaindl, Phys. Rev. B (Rapid Commun.) 31(1985)6836.
[44] H. Boppart and P. Wachter, Phys. Rev. Lett. 53(1984)1759;
H. Boppart, W. Rehwald, E. Kaldis and P. Wachter, in ref. [16], p. 81.
[45] J. Röhler, E. Dartyge, A. Fontaine, A. Jucha, K. Keulerz and D. Sayers, in ref. [4], p. 385.
[46] J. Moser, G.M. Kalvius and W. Zinn, Hyp. Int. 41(1988)499.
[47] M. Pasternak and R.D. Taylor, Hyp. Int. (1989), this volume.
[48] H.G. Zimmer, K. Takemura, K. Fischer and K. Syassen, Phys. Rev. B29(1984)2350.
[49] J. Röhler, Physica B144(1986)27.
[50] J.N. Farell and R.D. Taylor, Phys. Rev. Lett. 58(1987)2478;
R.D. Taylor and J.N. Farell, J. App. Phys. 61(1987)3669.
[51] C.M. Varma, Rev. Mod. Phys. 48(1976)219.
[52] I. Felner, I. Nowik, D. Vaknin, U. Potzel, J. Moser, G.M. Kalvius, G. Wortmann, G. Schmiester, G. Hilscher, E. Gratz, C. Schmitzer, N. Pillmayer, K.G. Prasad, H. de Waard and H. Pinto, Phys. Rev. B35(1987)6956.
[53] See refs. [7], [16], [17].
[54] E.V. Sampathkumaran, Hyp. Int. 28(1986)183.
[55] G. Kaindl, G.K. Wertheim, G. Schmiester and E.V. Sampathkumaran, Phys. Rev. Lett. 58(1987)606;
G. Kaindl and G.K. Wertheim, Phys. Rev. Lett. 61(1988)2629.
[56] G. Kaindl, G. Schmiester, E.V. Sampathkumaran and P. Wachter, Phys. Rev. B38(1988) 10174.
[57] G. Kalkowski, G. Kaindl, G. Wortmann, D. Lentz and S. Krause, Phys. Rev. B37(1988)1376.
[58] A. Kotani, T. Jo and J.C. Parlebas, Adv. Phys. 37(1988)37.
[59] G. Kaindl, G. Kalkowski, W.D. Brewer, E.V. Sampathkumaran, F. Holtzberg and A. Schach von Wittenau, J. Magn. Magn. Mater. 47 & 48(1985)181.
[60] D. Gignoux, F. Givord and J. Voivon, J. Less-Common Metals 94(1983)165;
D.Gignoux and J. Voivon, Phys. Rev. B32(1985)4822.
[61] T. Schedel, Diplom Thesis, Freie Universität Berlin (1987);
T. Schedel and G. Wortmann, HAYSLAB Annual Report 1987, p. 356;
T. Schedel et al., to be published.
[62] A. Bianconi, M. de Santis, A. DiCicco, A.M. Flank, A. Fontaine, P. Lagarde, H. Katayama-Yoshida, A. Kotani and A. Marcelli, Phys. Rev. B38(1988)7196.
[63] G. Kaindl, O. Strebel, A. Kolodziejczyk, W. Schäfer, R. Kiemel, S. Lösch, S. Kemmler-Sack, R. Hoppe, H.P. Müller and D. Kissel, in ref. [6], and to be published.
[64] B. Lengeler, M. Wilhelm, B. Jobst, W. Schwaen, B. Seebader and U. Hillebrecht, Solid State Commun. 65(1988)1545.
[65] See, for example, various contributions in ref. [6] and K.B. Garg et al., Phys. Rev. B38 (1988)244.
[66] J. Stöhr, in ref. [3].
[67] F. Sette, J. Stöhr and A.P. Hitchcook, J. Chem. Phys. 110(1984)577.
[68] J. Stöhr, F. Sette and A.L. Johnson, Phys. Rev. Lett. 53(1984)1684.

[69] G. Wortmann, W. Krone, V. Biebesheimer, G. Kaindl and S. Roth, Springer Tracts in Solid-State Science 63(1985)41.
[70] W. Krone, G. Wortmann and G. Kaindl, Synthetic Metals, in print;
G. Wortmann et al., Synthetic Metals 23(1988)139.
[71] G. Wortmann, W. Krone and G. Kaindl, in ref. [6].
[72] M. Tiedtke and G. Wortmann, Contribution to this conference.
[73] G. Schütz, M. Knülle, R. Wienke, W. Wilhelm, W. Wagner, P. Kienle and R. Frahm, Z. Phys. B73(1988)67.
[74] G. Schütz et al., in ref. [6] and HASYLAB Annual Report 1988, p. 201.